Barrier crossing in dissipative environments using the Non-Markovian Quantum Master Equation in the collective mode representation.

Anna Pomyalov and David Tannor
Dept. of Chemical Physics, The Weizmann Institute of Science,Rehovot, 76100 Israel

The calculation of chemical reaction rates in condensed phase is a central preoccupation of theoretical chemistry. At low temperatures, quantum mechanical effects can be significant and even dominant; yet quantum calculations of rate constants are extremely challenging, requiring theories and methods capable of describing quantum evolution in the presence of dissipation.

In this paper we present a new approach, based on the use of a non-Markovian quantum master equation (NM-QME). As opposed to other approximate quantum methods, the quantum dynamics of the system coordinate is treated exactly and hence there is no loss of accuracy at low temperatures. However, because of the perturbative nature of the NM-QME it breaks down for dimensionless frictions larger than about 0.1. We show that by augmenting the system coordinate with a collective mode of the bath, the regime of validity of the non-Markovian master equation can be extended significantly, up to dimensionless frictions of 0.5 over the entire temperature range. In the energy representation, the scaling goes as the number of levels in the relevant energy range to the 3rd power. This scaling is not prohibitive even for chemical systems with many levels, and hence we believe that the current method will find a useful place alongside the existing techniques for calculating quantum condensed phase rate constants.

PACS numbers:

I. INTRODUCTION

The calculation of chemical reaction rates in condensed phase is a central preoccupation of theoretical chemistry. For activated processes, the microscopic formulation of the rate involves the calculation of barrier crossing in the presence of dissipation induced by the environment. For many years, classical mechanics provided the only possible method to perform such calculations. Yet quantum effects can be important, particularly at temperatures below the so-called crossover temperature, where the activated process becomes exponentially small and quantum tunneling becomes dominant. The quantum process is particularly important in reactions involving light atoms, for example hydrogen transfer reactions, as well as in electronically non-adiabatic processes. Wolynes [1] calculated the quantum barrier crossing rate analytically for a parabolic barrier, essentially extending the classical memory friction result of Grote and Hynes [2] to the quantum regime. Subsequently, Pollak and Rips [3] developed an approximate theory of quantum barrier crossing that described the quantum mechanical counterpart of a Kramers' turnover in the transmission coefficient. About ten years ago, Topaler and Makri [4] provided the first exact quantum mechanical calculations for barrier crossing in solution as a function of friction and temperature. Their calculations have served ever since as a benchmark against which to compare approximate theories. However, the influence functional formalism of quantum dissipative dynamics [5–7], used in [4], is computationally costly, scaling exponentially with the number of time slices. As a result, much subsequent effort has gone into developing faster, albeit approximate methods for calculating quantum barrier crossing in the presence of dissipation.

In recent years, several methods have emerged that combine a quantum mechanical treatment of the equilibrium factors with a classical treatment of the dynamical evolution. Geva, Shi and Voth [8] and Shi and Geva [9] have developed an approximate method based on centroid molecular dynamics (CMD) that calculates the thermal flux contribution to the rate constant quantum mechanically but uses a classical approximation for the real time dynamics. Liao and Pollak [10] have developed a mixed classical-quantum method based on the use of the Wigner representation for the thermal flux combined with a classical approximation for the real time dynamics. The methods of [8–10] tend to be accurate at intermediate to high temperature, but deteriorate at low temperature where the classical treatment of the system dynamics begins to break down.

In this paper we present a new approach to calculating quantum rate constants based on the use of a non-Markovian quantum master equation (NM-QME). As opposed to other approximate quantum methods, the quantum dynamics of the system coordinate is treated exactly and hence there is no loss of accuracy in the low temperature regime. However, because of the perturbative nature of the NM-QME, it breaks down for dimensionless frictions larger than about 0.1. To overcome this limitation, the original NM-QME approach developed by Meier and Tannor [11] is reformulated in terms of the barrier normal modes (see, e.g. [10, 12]). The normal mode transformation allows one to express the system coordinate in terms of the unstable barrier mode coordinate

and the collective bath coordinate, making the system effectively two-dimensional. The unstable mode is (non-linearly) coupled to the collective bath mode, while the latter is coupled both to the unstable mode and to the harmonic bath. The explicit treatment of the collective bath mode amounts to replacing the density matrix of the original one-dimensional system with a density matrix for an extended two-dimensional system that includes the original system and the collective bath coordinate. However, the increase in the system size is accompanied by a significant reduction in the coupling strength to the residual bath, extending the range of validity of the non-Markovian master equation up to dimensionless frictions of 0.5 over the entire temperature range.

In coordinate space, the method scales as the 4th power of the number of grid points. However, a significant savings in obtained by working in the energy representation, where the scaling goes as the number of levels in the relevant energy range, N_l, to the 3rd power. This scaling is not prohibitive even for chemical systems with many system levels. For example, for the calculations in this paper on the double-well systems of ref. [4], N_l is up to 30 for the one-dimensinonal system and up to 100 for the extended two-dimensional system that includes the collective bath. Thus, we believe that the current method fills a useful niche alongside the techniques available for calculating condensed phase rate constants.

The outline of the paper is as follows. Section II provides a brief review of the NM-QME [11] (II B) as well as a review of the transformation of the Caldeira-Leggett Hamiltonian to the collective mode representation [10, 12] (II C). Section II D shows how the NM-QME may be combined with the flux-flux correlation function formulation to calculate quantum reaction rates. In Sect. III A we combine the formalisms of Sections II B and II C to obtain a set of equations for the NM-QME in the collective mode representation (QME-CM). All relevant parameters are derived for the specific example of the Drude spectral density in Sect. III B. In Section IV we discuss the effective two-dimensional potential, corresponding to the double well potential used in [4] (IV A) and give additional details of the computational method in the collective mode formulation (IV B). In Sect. V we present the results of rate constant calculations using both the original NM-QME and its collective mode variant. Section VI is a Conclusion.

II. PRELIMINARIES

A. A basic model

A widely used description of a system coupled to an environment is the Caldeira-Leggett Hamiltonian:

$$\boldsymbol{H} = \frac{\boldsymbol{p}^2}{2M} + W(\boldsymbol{x}) + \sum_{j=1}^{N}\Big[\frac{\boldsymbol{p}_j^2}{2m_j} + \frac{1}{2}m_j\omega_j\Big(x_j - \frac{\epsilon c_j}{m_j\omega_j}f(\boldsymbol{x})\Big)^2\Big]\,, \tag{2.1}$$

where $\boldsymbol{x}, \boldsymbol{p}$ and M are the coordinate, momentum and mass of the system; x_j, p_j and m_j are the coordinate, momentum and mass of the j-th bath oscillator ; ϵc_j is the coupling between the system and the j-th bath oscillator and $f(\boldsymbol{x})$ is some function of the system coordinate.

To emphasize the structure of the Hamiltonian that makes it convenient for the perturbation expansion we rewrite it in the following form:

$$\boldsymbol{H} = \boldsymbol{H}_s + \boldsymbol{H}_b + \epsilon\boldsymbol{H}_{sb} + \epsilon^2\boldsymbol{H}_{\rm ren}\,, \tag{2.2}$$

where we denote the free system Hamiltonian as

$$\boldsymbol{H}_s = \frac{\boldsymbol{p}^2}{2M} + V(\boldsymbol{x})\,, \tag{2.3}$$

the free bath Hamiltonian as

$$\boldsymbol{H}_b = \sum_{j=1}^{N}\Big[\frac{p_j^2}{2m_j} + \frac{1}{2}m_j\omega_j x_j\Big]\,, \tag{2.4}$$

the system-bath interaction term as

$$\boldsymbol{H}_{sb} = -\sum_{j=1}^{N} c_j x_j f(\boldsymbol{x})\,, \tag{2.5}$$

and the counter term as

$$\boldsymbol{H}_{\rm ren} = \frac{1}{2}\sum_{j=1}^{N}\frac{c_j^2}{m_j\omega_j^2}f(\boldsymbol{x})^2 = \frac{1}{2}\mu f(\boldsymbol{x})^2 \tag{2.6}$$

To characterize the bath, we introduce a spectral density of the bath oscillators:

$$J(\omega) = \frac{\pi}{2}\sum_{j=1}^{N}\frac{c_j}{m_j\omega_j}[\delta(\omega-\omega_j) - \delta(\omega+\omega_j)]\,, \tag{2.7}$$

where $\delta(x)$ is the Dirac delta-function. It is further convenient to define a complex bath correlation function

$$\begin{aligned} c(t) &= \int_{-\infty}^{\infty}\frac{d\omega}{2\pi}J(\omega)\cos(\omega t)\coth\Big(\frac{\beta\omega}{2}\Big) \\ &- i\int_{-\infty}^{\infty}\frac{d\omega}{2\pi}J(\omega)\sin(\omega t) = a(t) - ib(t)\,. \end{aligned} \tag{2.8}$$

B. The non-Markovian QME

The non-Markovian QME for the reduced density operator, as proposed in [11], is based on the second order perturbation expansion in coupling parameter ϵ of the total Hamiltonian, applied within the Nakajima-Zwanzig projection formalism [13]. It reads:

$$\begin{aligned} \dot\rho_{\rm s}(t) &= -i\mathcal{L}_{\rm s}^{\rm eff}\rho_{\rm s}(t) \\ &+ \epsilon^2\int_0^t dt'\mathcal{K}(t,t')\rho_{\rm s}(t') + \epsilon^2\int_{-\infty}^{0} dt'\mathcal{K}(t,t')\rho_{\rm s}^{\rm eq}\,. \end{aligned} \tag{2.9}$$

Here the reduced system density operator $\rho_{\rm s} = Tr_b(\rho)$ is obtained from the density operator of the global system by tracing out the bath degrees of freedom. The memory kernel $\mathcal{K}$ is given by

$$\mathcal{K}(t,t') = \mathcal{L}_-\Pi_{\rm s}(t,t')\Big[a(t-t')\mathcal{L}_- - ib(t-t')\mathcal{L}_+)\Big]\,, \quad (2.10)$$

where $a(t)$ and $b(t)$ are the real and imaginary parts of the bath correlation function, Eq.(2.8), and other entries are defined as follows:

$$\begin{aligned}
\Pi_{\rm s}(t,\ t_0) &= \mathcal{T}_+ e^{-i\int_{t_0}^t dt'\mathcal{L}_{\rm s}}\,, \quad \rho_{\rm s}^{\rm eq} = \frac{e^{-\beta \boldsymbol{H}_{\rm s}}}{Z_{\rm s}} \qquad (2.11)\\
\chi &= Tr_{\rm s}(f(\boldsymbol{x})e^{-\beta \boldsymbol{H}_{\rm s}})/Z_{\rm s}\,, \quad Z_{\rm s} = Tr_{\rm s}(e^{-\beta \boldsymbol{H}_{\rm s}})\,,\\
\mathcal{L}_{\rm s} &= \frac{1}{\hbar}[\boldsymbol{H}_{\rm s},\cdot]\,, \quad \mathcal{L}_- = \frac{1}{\hbar}[f(\boldsymbol{x}),\cdot]\,,\\
\mathcal{L}_+ &= \frac{1}{\hbar}[f(\boldsymbol{x})-\chi,\cdot]_+\,,\\
\mathcal{L}_{\rm s}^{\rm eff} &= \frac{1}{\hbar}[\boldsymbol{H}_s + \epsilon^2\frac{\mu}{2}[(f(\boldsymbol{x})-\chi)^2,\cdot]\,.
\end{aligned}$$

In Eq. (2.11), $\beta = (k_B T)^{-1}$, $[\cdot,\cdot]$ denotes a commutator, $[\cdot,\cdot]_+$ an anti-commutator and $\mathcal{T}_+$ a positive time ordering, applied when $\mathcal{L}_{\rm s}$ is explicitly time-dependent. The last term in Eq.(2.9) corresponds to the contribution of the system-bath correlations at time $t = 0$. The global system is assumed to be in thermal equilibrium for $t \le 0$, such that $\rho(0) = e^{-\beta \boldsymbol{H}}/Tr(e^{-\beta \boldsymbol{H}})$. The dynamics is induced at $t > 0$ by changing $\boldsymbol{H}_{\rm s}$.

A key feature of the efficient numerical solution of Eq. (2.9) [11] is the expansion of the bath correlation function, (2.8), in terms of a sum of complex exponents:

$$a(t) = \sum_{j=1}^{n_r}\alpha_j^r e^{-\gamma_j^r t}\,, \quad b(t) = \sum_{j=1}^{n_i}\alpha_j^i e^{-\gamma_j^i t}\,. \qquad (2.12)$$

It was shown in [11], that with (2.12) substituted into (2.10), Eq.(2.9) is equivalent to the following set of coupled equations for the primary density matrix $\rho_{\rm s}$ and for the auxiliary density matrices ρ_j^r and ρ_j^i:

$$\begin{aligned}
\dot\rho_{\rm s}(t) &= -i\mathcal{L}_{\rm s}^{\rm eff}\rho_{\rm s}(t) + \epsilon\mathcal{L}_-\Big(\sum_{j=1}^{n_r}\alpha_j^r\rho_j^r(t) - i\sum_{j=1}^{n_i}\alpha_j^i\rho_j^i(t)\Big)\,,\\
\dot\rho_j^r(t) &= \epsilon\mathcal{L}_-\rho_{\rm s}(t) - i(\mathcal{L}_{\rm s}+\gamma_j^r)\rho_j^r(t) \quad j = 1,...,n_r \quad (2.13)\\
\dot\rho_j^i(t) &= \epsilon\mathcal{L}_+\rho_{\rm s}(t) - i(\mathcal{L}_{\rm s}+\gamma_j^i)\rho_j^i(t) \quad j = 1,...,n_i\,,
\end{aligned}$$

with the auxiliary matrices defined as

$$\begin{aligned}
\rho_j^r(t) &= \epsilon\Big(\int_{-\infty}^t dt'\Pi(t,t')e^{-\gamma_j^r(t-t')}\mathcal{L}_-\rho_{\rm s}(t')\Big)\,, \quad (2.14)\\
\rho_j^i(t) &= \epsilon\Big(\int_{-\infty}^t dt'\Pi(t,t')e^{-\gamma_j^i(t-t')}\mathcal{L}_+\rho_{\rm s}(t')\Big)\,.
\end{aligned}$$

In this definition we combined the last two terms in Eq.(2.9), assuming explicitly that the system was in thermal equilibrium at $t \le 0$.

C. Derivation of the Hamiltonian in the collective mode representation.

For the sake of completeness we repeat here the derivation of the Hamiltonian in the collective mode representation, following Ref.[10].

To apply the normal mode transformation we limit ourselves to a one-dimensional double-well potential and rewrite the original Hamiltonian (2.1) for the system by defining a mass-weighted system coordinate $q = xM^{-1/2}$ bilinearly coupled to a bath of harmonic oscillators with mass-weighted coordinates $x_j m_j^{-1/2}$:

$$H = \frac{1}{2}p_q^2 + W(q) + \frac{1}{2}\sum_j\Big[p_j^2 + \Big[(\omega_j x_j - \frac{c_j}{\omega_j}q\Big)^2\Big] \quad (2.15)$$

For future use we define here the mass-independent bath friction function

$$\gamma(t) = \frac{1}{M}\sum_j\frac{c_j^2}{\omega_j^2}\cos(\omega_j t)\,, \qquad (2.16)$$

related to the spectral density of the bath oscillators, Eq.(2.7), as:

$$\gamma(t) = \frac{2}{M}\int_0^\infty\frac{d\omega}{\pi}\frac{J(\omega)}{\omega}\cos(\omega t) \qquad (2.17)$$

and its Laplace transform

$$\hat\gamma(s) = \int_0^\infty dt e^{-st}\gamma(t) = \frac{1}{M}\int_0^\infty\frac{d\omega}{\pi}\frac{J(\omega)}{\omega}\frac{2s}{\omega_j^2+s^2}\,. \qquad (2.18)$$

The potential $W(q)$ is assumed to have two wells at $q = \pm q_0$ and a barrier at $q = q^\ddagger$. One may expand the potential around the barrier top:

$$W(q) = W(q^\ddagger) - \frac{1}{2}{\omega^\ddagger}^2(q-q^\ddagger)^2 + W_1(q)\,. \qquad (2.19)$$

This expansion defines the barrier frequency $\omega^\ddagger$ and the non-linear part of the potential, $W_1(q)$.

Discarding the non-linear part of the potential, we get a quadratic in all coordinates and momenta Hamiltonian, that may be diagonalized using the normal mode transformation [14, 15]. In was shown in [14], that the barrier frequency is determined by the Laplace transform of the time-dependent friction through the Kramers-Grote-Hynes equation:

$${\lambda^\ddagger}^2 + \lambda^\ddagger\hat\gamma(\lambda^\ddagger) = {\omega^\ddagger}^2\,, \qquad (2.20)$$

where $-{\lambda^\ddagger}^2$ is a negative eigenvalue of the force constant matrix at the barrier. We denote the coordinate associated with this eigenvalue as ℓ, and the coordinates associated with the positive eigenvalues λ_j^2 as $y_j : j = 1,...,N$, where N is the number of bath modes.

One can express the system coordinate in terms of the barrier normal modes as:

$$q = u_{00}\ell + \sum_{j=1}^{N} u_{j0} y_j \,, \tag{2.21}$$

where the u_{ij} are matrix elements of the transformational matrix that diagonalizes the barrier force constant matrix.

The parabolic Hamiltonian may be expressed in terms of normal modes as

$$\boldsymbol{H}_{\rm par} = \frac{1}{2}\Big(p_\ell^2 + \sum_{j=1}^{N} p_{y_j}^2 - \lambda^{\ddagger\,2}\ell^2 + \sum_{j=1}^{N}\lambda_j^2 y_j^2\Big)\,. \tag{2.22}$$

One may define a collective bath mode σ as

$$\sigma = \frac{1}{u_1}\sum_{j=1}^{N} u_{j0} y_j \,, \quad u_1^2 \equiv \sum_{j=1}^{N} u_{j0}^2 = 1 - u_{00}^2. \tag{2.23}$$

The matrix element u_{00} may be expressed in the continuum limit in terms of the Laplace transform of the friction function as [16]

$$u_{00}^2 = \Big(1 + \frac{1}{2}\Big(\frac{\hat{\gamma}(\lambda^\ddagger)}{\lambda^\ddagger} + \frac{\partial\hat{\gamma}(s)}{\partial s}\Big|_{s=\lambda^\ddagger}\Big)\Big)^{-1} \tag{2.24}$$

With this definition, the original Hamiltonian may be rewritten in terms of the new set of coordinates $\ell, \sigma, \boldsymbol{r}$ as [10]

$$\begin{aligned}\boldsymbol{H} &= \frac{1}{2}(p_\ell^2 + p_\sigma^2 - \lambda^{\ddagger\,2}\ell^2 + \omega_\sigma^2\sigma^2) + W_1[q(\ell,\sigma)] \\ &+ \frac{1}{2}\sum_j \Big[p_{r_j}^2 + \Big(\omega_j r_j - \frac{h_j}{\omega_j}\sigma\Big)^2\Big]\,.\end{aligned} \tag{2.25}$$

where $\lambda^\ddagger$ is defined by Eq.(2.20), the bath collective mode frequency by

$$\omega_\sigma^{-2} = \frac{1}{u_1^2}\sum_{j=1}^{N}\frac{u_{j0}^2}{\lambda_j^2}\,, \tag{2.26}$$

and h_j are the system-bath coupling constants in the new coordinate system. The friction function for the collective bath mode is given by:

$$\gamma_\sigma(t) = \sum_{j=1}^{N}\frac{h_j^2}{\omega_j^2}\cos(\omega_j t)\,. \tag{2.27}$$

From $\gamma_\sigma(t)$ one can calculate the new spectral density using eq. 2.17, and then the new complex bath correlation function from eq. 2.8. It can be shown [10] that all the parameters of eq. 2.25, and therefore $\gamma_\sigma(t)$ as well, are completely determined in the continuum limit by $\gamma(t)$ or alternatively by $\hat{\gamma}(s)$.

In practice, in our method $\gamma_\sigma(t)$ is actually calculated via the inverse Laplace transform of $\hat{\gamma}_\sigma(t)$. The latter is given by [10]

$$\hat{\gamma}_\sigma(s) = s\Big(\frac{u_1^2\sum_{j=1}^{N}\frac{u_{j0}^2}{\lambda_j^2(\lambda_j^2+s^2)}}{\sum_{j=1}^{N}\frac{u_{j0}^2}{\lambda_j^2}\sum_{j=1}^{N}\frac{u_{j0}^2}{\lambda_j^2+s^2}}\Big) \tag{2.28}$$

As shown in [10], by using the identity

$$\frac{u_{00}^2}{-\lambda^{\ddagger\,2}+s^2} + \sum_{j=1}^{N}\frac{u_{j0}^2}{\lambda_j^2+s^2} = [-\omega^{\ddagger\,2} + s^2 + s\hat{\gamma}(s)]^{-1}\,, \tag{2.29}$$

together with eqs. (2.20),(2.23), (2.24), eq.(2.28) can be expressed in the continuum limit entirely as a function of s, $\hat{\gamma}(s)$ and $\omega^\ddagger$.

The inverse Laplace transform of $\hat{\gamma}_\sigma(s)$ required in our method can be tricky. Laplace transforms are very delicate to handle numerically, and analytical inverse Laplace transforms exist for only a limited class of functions. As a result, our method is best suited for friction functions $\gamma(t)$ which lead to a form of $\hat{\gamma}_\sigma(s)$ that is analytically invertible. In contrast, in the MQCLT method used in [10], the reaction rates are defined directly through the Laplace transform of the new friction function $\hat{\gamma}_\sigma(s)$ itself, and thus does not require its inversion.

D. Reaction rate constant from flux-flux correlation function.

The quantum mechanically exact expression for a thermal rate constant can be written in terms of the flux correlation function

$$k(T) = Q_0^{-1}\lim_{t\to\infty} C_{fs}(t)\,, \tag{2.30}$$

where $Q_0(T)$ is the reactant partition function per unit volume and $C_{fs}(t)$ is the flux-side correlation function

$$C_{fs}(t) = Tr[e^{-\beta\boldsymbol{H}}\boldsymbol{F}\mathcal{P}]\,. \tag{2.31}$$

Here $\boldsymbol{F}$ is the bare flux operator

$$\boldsymbol{F} = \frac{i}{\hbar}[\boldsymbol{H}, h(\boldsymbol{s})]_{s=0}\,, \tag{2.32}$$

s is the reaction coordinate, $h(\boldsymbol{s})$ is the Heaviside step function, equal to 0(1) on reactants(products) side of the dividing point, defined by $s=0$, and $\beta = (k_{\rm B}T)^{-1}$ is the inverse temperature.

The projection operator $\mathcal{P}$ is defined by:

$$\mathcal{P} = e^{i\boldsymbol{H}t}h(\boldsymbol{p})e^{-i\boldsymbol{H}t}\,, \tag{2.33}$$

with $\boldsymbol{p}$ the momentum operator. Using these definitions explicitly, the flux-side correlation function may be written as:

$$C_{fs}(r;t) = Tr[\hat{F}(\beta)e^{i\boldsymbol{H}t/\hbar}\boldsymbol{h}e^{-i\boldsymbol{H}t/\hbar}]\,, \tag{2.34}$$

where $\boldsymbol{F}(\beta) = e^{-\beta \boldsymbol{H}} \boldsymbol{F}$ is the Bolzmannized flux operator.

It was shown by Miller that the rate constant may be equivalently expressed via a time integral of the flux-flux autocorrelation function

$$Q_0(T)k(T) = \int_0^\infty dt C_{ff}(t) \quad (2.35a)$$

$$C_{ff}(t) = Tr[\boldsymbol{F}(\beta) e^{i\boldsymbol{H}t} \boldsymbol{F} e^{-i\boldsymbol{H}t}] , \quad (2.35b)$$

$$Q_0(T) = Tr[e^{-\beta \boldsymbol{H}} \boldsymbol{h}]. \quad (2.35c)$$

The Boltzmannized flux operator may be written in different ways. The simplest one is $\hat{F}(\beta) = e^{-\beta \boldsymbol{H}} \boldsymbol{F}$. Performing a cyclic permutation of $e^{-\beta \boldsymbol{H}}$ within the trace of Eq. (2.35b) it may be "half-split" once

$$\boldsymbol{F}(\beta) = e^{-\beta \boldsymbol{H}/2} \boldsymbol{F} e^{\beta \boldsymbol{H}/2} \quad (2.36)$$

or twice

$$\boldsymbol{F}(\beta/2) = e^{-\beta \boldsymbol{H}/4} \boldsymbol{F} e^{-\beta \boldsymbol{H}/4} \quad (2.37)$$

to give a symmetric form of C_{ff}(2.35b):

$$C_{ff}(t) = Tr[\boldsymbol{F}(\beta/2) e^{i\boldsymbol{H}t} \boldsymbol{F}(\beta/2) e^{-i\boldsymbol{H}t}] . \quad (2.38)$$

Another variant of the flux operator is the Kubo form:

$$\boldsymbol{F}_{\rm Kubo}(\beta) = \frac{1}{\beta} \int_0^\beta d\lambda e^{-(\beta-\lambda)\boldsymbol{H}} \boldsymbol{F}(\boldsymbol{s}) e^{\lambda \boldsymbol{H}} \quad (2.39)$$

$$= \frac{i}{\hbar\beta} [\boldsymbol{h}, e^{-\beta \boldsymbol{H}}] .$$

These formulae may be combined to give a smooth interpolation between the half-split and Kubo forms [19]:

$$\boldsymbol{F}_\kappa(\beta) = \frac{i}{\hbar\kappa\beta} [e^{-(1-\kappa)\beta\boldsymbol{H}/2} \boldsymbol{h} e^{-(1+\kappa)\beta\boldsymbol{H}/2} \quad (2.40)$$

$$- e^{-(1+\kappa)\beta\boldsymbol{H}/2} \boldsymbol{h} e^{-(1-\kappa)\beta\boldsymbol{H}/2}]$$

with $0 < \kappa < 1$. This form reduces to the Kubo formula for $\kappa \to 1$ and to the half-split form for $\kappa \to 0$. Different forms have advantages and disadvantages for different methods of propagation and at different temperatures.

As a first step, we use Eq.(2.38) with the intermediate form of the Boltzmannized flux ($\kappa = 1/2$)

$$\boldsymbol{F}_{\rm inter}(\beta) = \frac{2i}{\hbar\beta} [e^{-(\beta\boldsymbol{H}/4} \boldsymbol{h} e^{-3\beta\boldsymbol{H}/4} \quad (2.41)$$

$$- e^{-3\beta\boldsymbol{H}/4} \boldsymbol{h} e^{-\beta\boldsymbol{H}/4}]$$

It was shown in [19] that this form of the Boltzmannized flux has a particulary smooth shape in the coordinate representation and leads to fast convergence of the integral.

Assuming factorized initial conditions, we can split the trace in (2.38) into two parts:

$$C_{ff}(t) = Tr_{\rm s} \boldsymbol{F}_{\rm s}(\beta/2) \{Tr_{\rm b}[e^{-i\boldsymbol{H}t} \boldsymbol{F}_{\rm inter}(\beta/2) e^{i\boldsymbol{H}t}]\}$$

$$= Tr_{\rm s}\{\boldsymbol{F}_{\rm s}(\beta/2) \mathcal{F}(t, \beta/2)\} , \quad (2.42)$$

where

$$\boldsymbol{F}_{\rm s}(\beta) = \frac{2i}{\hbar\beta} [e^{-(\beta \boldsymbol{H}_{\rm s}/4} \boldsymbol{h} e^{-3\beta \boldsymbol{H}_{\rm s}/4} \quad (2.43a)$$

$$- e^{-3\beta \hat{H}_{\rm s}/4} \hat{h} e^{-\beta \hat{H}_{\rm s}/4}]$$

$$\mathcal{F}(t, \beta) = Tr_{\rm b}[e^{-i\boldsymbol{H}t} \boldsymbol{F}_{\rm inter}(\beta) e^{i\boldsymbol{H}t}] . \quad (2.43b)$$

If we consider $\boldsymbol{F}_{\rm inter}(\beta)$ as a (un-normalized) density matrix of the global system, then $\mathcal{F}(t, \beta)$ is the corresponding reduced density matrix of the system. It may be calculated by solving the Nakajima-Zwanzig equation (in the Non-Markovian QME formulation). The initial conditions are

$$\mathcal{F}(0, \beta) = \boldsymbol{F}_{\rm s}(\beta) , \quad (2.44)$$

where $\boldsymbol{F}_{\rm s}(\beta)$, Eq(2.43a), is defined via the un-normalized equilibrium system density matrix $e^{-\beta \boldsymbol{H}_{\rm s}}$, and the auxiliary matrices are initially set to zero.

The reaction rate constant is calculated as a plateau value of the integral of the flux-flux correlation function:

$$k(t, T) = \frac{1}{Q_0(T)} \int_0^t dt' C_{ff}(t'), \quad (2.45)$$

and the transmission coefficient is the ratio of $k(t)$ to a classical transition rate theory result

$$k_{\rm TST} = \frac{\omega_0}{2\pi} e^{-\beta E_b} , \quad (2.46)$$

where ω_0 is the well frequency and E_b is the barrier height.

III. NON-MARKOVIAN QME IN COLLECTIVE MODE REPRESENTATION

A. QME in collective mode representation

One may consider Eq. (2.25) as a particular case of Eq.(2.1), where the system coordinate $\boldsymbol{x}$ has two components $\boldsymbol{x} = (\ell, \sigma)$ and the function $f(\boldsymbol{x})$ in the coupling term is just σ. The coupling constants h_j of the bath oscillators contain some expansion parameter $\tilde{\epsilon}$ with yet unknown relation to ϵ.

The Nakajima-Zwanzig projection formalism [13] is not limited to one-dimensional systems. Applying it to the evolution of the system described by Eq.(2.25) we receive the following set of equations:

$$\dot{\rho}_{\rm s}(\ell, \ell', \sigma, \sigma'; t) = -i\tilde{\mathcal{L}}_{\rm s}^{\rm eff} \rho_{\rm s}(\ell, \ell', \sigma, \sigma'; t) \quad (3.1a)$$

$$+\tilde{\epsilon}^2 \int_0^t dt' \tilde{\mathcal{K}}(t, t') \rho_{\rm s}(\ell, \ell', \sigma, \sigma'; t') + \tilde{\epsilon}^2 \int_{-\infty}^0 dt' \tilde{\mathcal{K}}(t, t') \rho_{\rm s}^{\rm eq} ,$$

$$\tilde{\mathcal{K}}(t, t') = \tilde{\mathcal{L}}_- \tilde{\Pi}_{\rm s}(t, t') \Big[\tilde{a}(t - t') \tilde{\mathcal{L}}_- - i\tilde{b}(t - t') \tilde{\mathcal{L}}_+)\Big] , \quad (3.1b)$$

where we have written the coordinate dependence of the density matrix explicitly and defined the following quantities by analogy with Eq.(2.11):

$$\tilde{\Pi}_{\rm s}(t,\ t_0) = \mathcal{T}_+ e^{-i\int_{t_0}^{t'} dt' \tilde{\mathcal{L}}_{\rm s}}\,, \quad \rho_{\rm s}^{\rm eq} = \frac{e^{-\beta \boldsymbol{H}_{\rm s}}}{Z_{\rm s}} \tag{3.2}$$

$$\chi = Tr_{\rm s}(\sigma e^{-\beta \boldsymbol{H}_{\rm s}})/Z_{\rm s}\,, \quad Z_{\rm s} = Tr_{\rm s}(e^{-\beta \boldsymbol{H}_{\rm s}})\,,$$

$$\tilde{\mathcal{L}}_{\rm s} = \frac{1}{\hbar}[\boldsymbol{H}_{\rm s}, \cdot]\,, \quad \tilde{\mathcal{L}}_- = \frac{1}{\hbar}[\sigma, \cdot]\,,$$

$$\tilde{\mathcal{L}}_+ = \frac{1}{\hbar}[\sigma - \chi, \cdot]_+\,,$$

$$\tilde{\mathcal{L}}_{\rm s}^{\rm eff} = \frac{1}{\hbar}[\boldsymbol{H}_s + \tilde{\epsilon}^2 \frac{\mu}{2}[(\sigma-\chi)^2, \cdot]\,,$$

$$\boldsymbol{H}_{\rm s} = \frac{1}{2}(p_\ell^2 + p_\sigma^2 - {\lambda^\ddagger}^2 \ell^2 + \omega_\sigma^2 \sigma^2) + W_1[q(\ell,\sigma)].\,,$$

The parameters of $\boldsymbol{H}_{\rm s}$ are defined in the previous section. The functions $\tilde{a}(t-t')$ and $\tilde{b}(t-t')$ in (3.1b) are the real and imaginary parts of the bath correlation function with the bath spectral density, $\tilde{J}(\omega)$, recovered from the collective mode friction function γ_σ by

$$\tilde{J}(\omega) = \omega \int_0^\infty dt \gamma_\sigma(t) \cos(\omega t) \tag{3.3}$$

and expanded in a new sum of exponents, as in Eq.(2.12).

The non-local in time Eq. (3.1) may be rewritten as before as a set of coupled simultaneous equations:

$$\dot{\rho}_{\rm s}(\ell,\ell',\sigma,\sigma';t) = -i\tilde{\mathcal{L}}_{\rm s}^{\rm eff}\rho_{\rm s}(\ell,\ell',\sigma,\sigma';t) + \tilde{\epsilon}\tilde{\mathcal{L}}_-\Big(\sum_{j=1}^{n_r}\tilde{\alpha}_j^r\rho_j^r(t) - i\sum_{j=1}^{n_i}\tilde{\alpha}_j^i\rho_j^i(t)\Big)\,, \tag{3.4}$$

$$\dot{\rho}_j^r(t) = \tilde{\epsilon}\tilde{\mathcal{L}}_-\rho_{\rm s}(\ell,\ell',\sigma,\sigma';t) - i(\tilde{\mathcal{L}}_{\rm s} + \tilde{\gamma}_j^r)\rho_j^r(t)\,,\ j=1,\ldots,n_r$$

$$\dot{\rho}_j^i(t) = \tilde{\epsilon}\tilde{\mathcal{L}}_+\rho_{\rm s}(\ell,\ell',\sigma,\sigma';t) - i(\tilde{\mathcal{L}}_{\rm s} + \tilde{\gamma}_j^i)\rho_j^i(t)\,,\ j=1,\ldots,n_i\,,$$

with the auxiliary matrices defined as:

$$\rho_j^r(t) = \tilde{\epsilon}\Big(\int_{-\infty}^t dt' \tilde{\Pi}(t,t') e^{-\tilde{\gamma}_j^r(t-t')}\tilde{\mathcal{L}}_-\rho_{\rm s}(t')\Big)\,, \tag{3.5}$$

$$\rho_j^i(t) = \tilde{\epsilon}\Big(\int_{-\infty}^t dt' \tilde{\Pi}(t,t') e^{-\tilde{\gamma}_j^i(t-t')}\tilde{\mathcal{L}}_+\rho_{\rm s}(t')\Big)\,.$$

The evolution of the primary density matrix is affected by the bath via $\mathcal{L}_-$, which depends only on σ, while the evolution of the auxiliary matrices include the terms with $\mathcal{L}_{\rm s}$, that depend on both ℓ and σ.

B. Calculation of the Parameters of the Hamiltonian

We continue our analysis by specifying the spectral density for the original harmonic bath. We start by calculating the set of parameters of the two-dimensional Hamiltonian, Eq.(2.25), defined by equations (2.20),(2.23),(2.24),(2.26) and (2.28). Next, we have to recover a spectral density of a newly defined harmonic bath using relation (3.3) to extract a new expansion parameter and to calculate the bath correlation function $\tilde{c}(t) = \tilde{a}(t) + i\tilde{b}(t)$, Eq.(2.8). As a last step, we expand $\tilde{a}(t)$ and $\tilde{b}(t)$ in a set of complex exponents and calculate all $\tilde{\alpha}^{r,i}$'s and $\tilde{\gamma}^{r,i}$'s.

To set a reference against which to check the calculations, we start with the simplest example, the Ohmic spectral density

$$J(\omega) = \frac{\epsilon}{M}\omega = \gamma\omega\,. \tag{3.6}$$

The corresponding friction function is $\gamma(t) = \gamma\delta(t)$. Its Laplace transform is just $\hat{\gamma}(s) = \gamma$. Then, the effective barrier frequency $\lambda^\ddagger$ is calculated analytically from ${\lambda^\ddagger}^2 + \gamma\lambda^\ddagger - {\omega^\ddagger}^2 = 0$ and

$$u_{00}^2 = 2\lambda^\ddagger/(2\lambda^\ddagger + \gamma) \quad u_1^2 = \gamma/(2\lambda^\ddagger + \gamma)\,. \tag{3.7}$$

The collective bath mode frequency, (2.26), is calculated by setting $s=0$ in Eq.(2.29) which gives the simple result $\omega_\sigma^2 = {\omega^\ddagger}^2$. Finally, using (2.20),(2.26) and (2.28) we arrive at

$$\hat{\gamma}_\sigma(s) = \gamma + 2\lambda^\ddagger\,. \tag{3.8}$$

This simple spectral density is, however, not useful for realistic calculations. Ideally, we should use the same spectral density as Topaler and Makri, [4], the Ohmic with exponential cutoff

$$J(\omega) = \epsilon\omega e^{-\omega/\omega_c}\,. \tag{3.9}$$

Unfortunately, the resulting $\hat{\gamma}_\sigma(s)$ is not amenable to analytic inversion.

Instead, we use the so-called Drude spectral density

$$J(\omega) = \epsilon\omega/(1+(\omega/\omega_c)^2)\,, \tag{3.10}$$

which corresponds to an exponential friction function with a cutoff in the time domain:

$$\gamma(t) = \frac{\gamma}{\tau}e^{-t/\tau}\,, \quad \tau = \omega_c^{-1}\,. \tag{3.11}$$

Its Laplace transform

$$\hat{\gamma}(s) = \gamma/(1+s\tau) \tag{3.12}$$

reduces to the Ohmic case for $\tau \to 0$. We therefore will use this limit to check our results, where possible.

We start with $\lambda^\ddagger$. Eq.(2.20) becomes a cubic equation for $\lambda^\ddagger$ and does not have a simple analytical solution. We therefore will express all the Hamiltonian parameters in terms of $\hat{\gamma}_\lambda \equiv \hat{\gamma}(\lambda^\ddagger)$ and the actual values will be calculated later numerically for the specific parameters of the potential and the coupling strength γ.

According to Eqs.(2.23) and (2.24)

$$u_{00}^2 = \frac{2\gamma\lambda^\ddagger}{2\gamma\lambda^\ddagger + \hat{\gamma}_\lambda^2}\,, \quad u_1^2 = \frac{\hat{\gamma}_\lambda^2}{2\gamma\lambda^\ddagger + \hat{\gamma}_\lambda^2}\,. \tag{3.13}$$

To check the result,we note that in the Ohmic case $\hat{\gamma}_\lambda = \gamma$. Substituting this relation into (3.13) we arrive at the Ohmic results given above.

For the collective mode frequency we get

$$\omega_\sigma^2 = \frac{\omega^{\ddagger 2}}{1+2\lambda^\ddagger\tau}\,, \tag{3.14}$$

which for $\tau \to 0$ coincides with the Ohmic result. An elaborate analysis leads to the collective mode friction function in the following form:

$$\hat{\gamma}_\sigma(s) = \frac{\gamma + 2\lambda^\ddagger(1+\lambda^\ddagger\tau)^2}{(1+\lambda^\ddagger\tau)(1+s\tau+2\lambda^\ddagger\tau)}\,. \tag{3.15}$$

that clearly goes to $\gamma + 2\lambda^\ddagger$ at $\tau \to 0$. This function may be inverted, giving the friction function in the time domain

$$\gamma_\sigma(t) = \frac{e^{-t(1+2\lambda^\ddagger\tau)/\tau}(\gamma + 2\lambda^\ddagger(1+\lambda^\ddagger\tau)^2)}{\tau(1+2\lambda^\ddagger\tau)}\,. \tag{3.16}$$

Comparing with the form of the original friction function we find that $\gamma_\sigma(t)$, Eq.(3.11) may be rewritten as:

$$\gamma_\sigma(t) = \frac{\tilde{\epsilon}}{\tilde{\tau}}e^{-t/\tilde{\tau}}\,, \quad \tilde{\epsilon} = \frac{\gamma + 2\lambda^\ddagger(1+\lambda^\ddagger\tau)^2}{(1+2\lambda^\ddagger\tau)^2}\,, \quad \tilde{\tau} = \frac{\tau}{1+2\lambda^\ddagger\tau}\,. \tag{3.17}$$

Such a simple functional form allows us to immediately recover the spectral density of the new harmonic bath:

$$\tilde{J}(\omega) = \frac{\tilde{\epsilon}\omega}{1+(\omega/\tilde{\omega}_c)^2}\,, \quad \tilde{\omega}_c = \omega_c + 2\lambda^\ddagger, \tag{3.18}$$

a result that was verified by a direct calculation.

As a result of the transformation, the cutoff frequency becomes higher by twice the effective barrier frequency, and the coupling strength has changed. The behavior of the renormalized coupling is quite interesting. For very small γ,

$$\tilde{\epsilon} \to \frac{2\omega^\ddagger(1+\omega^\ddagger\tau)^2}{(1+2\omega^\ddagger\tau)^2} \tag{3.19}$$

and it grows slower than γ, since $\lambda^\ddagger$ itself decreases with γ. It will be used as a new expansion parameter in the Hamiltonian. In the limit $\gamma \to 0$ all λ_j's are equal to zero and the unstable mode ℓ coincides with the original coordinate [14].

The bath correlation function (2.8) was calculated by contour integration and recast in the exponential expansion (2.12). We obtain

$$\tilde{a}(t) = \frac{\tilde{\omega}_c}{2}\coth\Big[\frac{\beta\hbar\tilde{\omega}_c}{2}\Big]e^{-\tilde{\omega}_c t} + \frac{2}{\beta\hbar}\sum_n^\infty \frac{\nu_n}{\nu_n^2/\tilde{\omega}_c^2 - 1}e^{-\nu_n t}\,, \tag{3.20a}$$

$$\tilde{b}(t) = -\frac{\tilde{\omega}_c}{2}e^{-\tilde{\omega}_c t}\,, \tag{3.20b}$$

where $\nu_n = (2\pi)/(\beta\hbar)$ are the Matsubara frequencies, $\tilde{\omega}_c$ is defined in (3.18), and the common factor $\tilde{\epsilon}$ has been omitted.

TABLE I: parameters of the DW1 potential

units	$E^\ddagger$	$\omega^\ddagger$	ω_0	ω_c
cm^{-1}	2085	500	707	500
a.u.	9.508×10^{-3}	2.278×10^{-3}	3.224×10^{-3}	2.28×10^{-3}

IV. COMPUTATIONAL DETAILS

A. Parameters of the potential.

The double-well potential that we use is DW1 used in [4]

$$W(q) = -\frac{m_0\omega^{\ddagger 2}}{2}q^2 + \frac{m_0^2\omega^{\ddagger 4}}{16E^\ddagger}q^4\,, \tag{4.1}$$

with parameters given in Table I.

The mass of the system coordinate (proton) is $m_0 = 1836.46$ a.u. A dimensionless dissipation parameter $\gamma_{\rm rel} = \epsilon/m_0\omega^\ddagger$ was used to characterize the coupling strenth with the bath.

In the mass-weighted form that we used for the normal mode transformation the potential reads:

$$W(q) = -\frac{\omega^{\ddagger 2}}{2}q^2 + \frac{\omega^{\ddagger 4}}{16E^\ddagger}q^4\,, \tag{4.2}$$

where $E^\ddagger$ is the barrier height. Comparing with Eq.(2.19), we find that the barrier of the potential is at $q^\ddagger = 0$ and the non-linear part is just

$$W_1(q) = \frac{\omega^{\ddagger 4}}{16E^\ddagger}q^4\,. \tag{4.3}$$

To match the conditions of [4], we use the dimensionless friction coefficient

$$\gamma_{\rm rel} = \frac{\gamma}{\omega^\ddagger}\,. \tag{4.4}$$

as a starting point in the calculation of parameters. For each $\gamma_{\rm rel}$ we calculate $\gamma = \gamma_{\rm rel}\omega^\ddagger$. Then using (2.20) and (3.12) we calculate $\lambda^\ddagger$. Having $\lambda^\ddagger$ we repeat all steps in Sect.III B, i.e. Eqs.(3.13),(3.17),(3.18) and (3.20). Next, we express the original coordinate q in the normal mode coordinates: $q = u_{00}\ell + u_1\sigma$ and rewrite the potential as

$$W(\ell,\sigma) = \frac{1}{2}\Big(-\lambda^{\ddagger 2}\ell^2 + \omega_\sigma^2\sigma^2\Big) + \frac{\omega^{\ddagger 4}}{16E^\ddagger}(u_{00}\ell + u_1\sigma)^4\,. \tag{4.5}$$

The parameters of the potential for a number of $\gamma_{\rm rel}$ are given in Table II.

The contours of the potential for $\gamma_{\rm rel} = 0.05, 0.5$ and 1 are shown in Fig.1. The rotation of the potential in the $\ell-\sigma$ plane is evident, reflecting the increasing role of the collective mode in the system with increasing system-bath coupling strength.

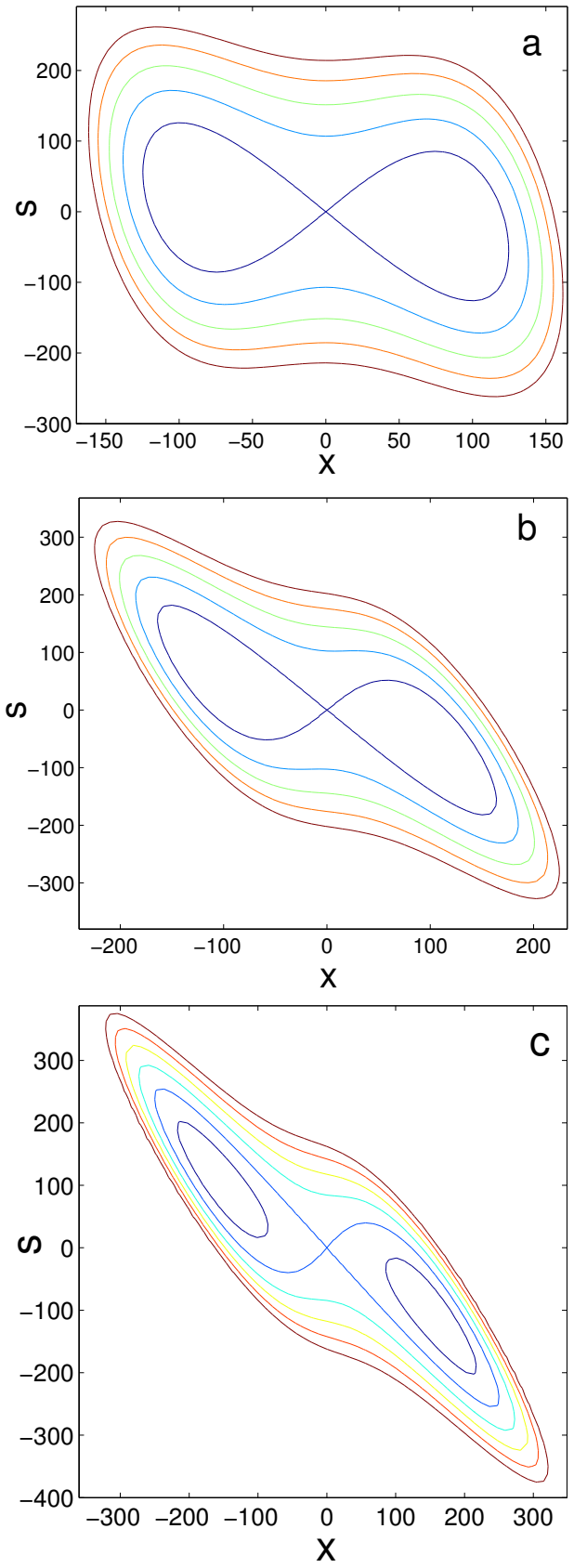

FIG. 1: The contours of the two-dimensional potential for (a) $\gamma_{\rm rel} = 0.05$, (b) $\gamma_{\rm rel} = 0.5$, and (c) $\gamma_{\rm rel} = 1$. The coordinate ℓ and σ are marked as x and s in the figures.

TABLE II: parameters of the potential in (4.5)

$\gamma_{\rm rel}$	$\lambda^{\ddagger 2}$	ω_σ^2	u_{00}	u_1
0.05	5.061×10^{-6}	1.744×10^{-6}	0.997	0.079
0.1	4.936×10^{-6}	1.759×10^{-6}	0.993	0.114
0.5	4.039×10^{-6}	1.877×10^{-6}	0.962	0.272
1	3.138×10^{-6}	2.031×10^{-6}	0.911	0.411
2	1.867×10^{-6}	2.359×10^{-6}	0.778	0.628
5	2.762×10^{-7}	3.551×10^{-6}	0.350	0.937
10	8.875×10^{-8}	4.113×10^{-6}	0.179	0.983

B. The time propagation

To calculate the rates we have to calculate the flux operator $\hat{\mathcal{F}}(t,\beta)$ as a function of time. The general strategy is the same for NM-QME and its collective mode version, QME-CM.

The flux-flux correlation function, $C_{ff}(t)$, was defined via $\hat{\mathcal{F}}(t,\beta)$ [cf. (2.43b)], which can be viewed as an (un-normalized) reduced density matrix. The Hamiltonian is first build on a grid using the discrete variable representation [20]. Even with a modest number of points in each direction the calculation is challenging, especially for low temperatures, due to the large number of $N \times N$ primary and auxiliary density matrices. The difficulty is particularly acute for the QME-CM case (3.4), for which the size of the matrices is $N^2 \times N^2$. On the other hand, at low temperatures, only limited number of energy levels is populated. We will use this advantage to facilitate the calculations.

We choose the energy representation for calculating the time evolution of $\hat{\mathcal{F}}(t,\beta)$ using a relatively small number of states.

The initial state is prepared as a flux operator (2.41,2.43b), built using an (un-normalized) equilibrium thermal density matrix $e^{-\beta \hat{E}_n}$. We then use the Short Iterative Arnoldi [18] or $4^{\rm th}$ -order Runge-Kutta method to propagate the flux operator $\hat{\mathcal{F}}(t,\beta)$ in time according to (2.13) and (3.4), with all auxiliary matrices initially set to zero. The flux-flux correlation function $Tr_{\rm s}\{\hat{F}_{\rm s}(\beta/2)\hat{\mathcal{F}}(t,\beta/2)\}$ is calculated as a function of time. Here, trace over the system for the QME-CM is understood to be over both system degrees of freedom.

Although for the NM-QME (2.13) the construction of the Hamiltonian matrix and its diagonalization is a standard procedure, it is more complicated for the QME-CM case (3.4). We therefore give the details of these calculations.

We start with the calculation of the matrix elements of the system Hamiltonian on a two-dimensional grid (ℓ,σ):

$$\boldsymbol{H}_s(\ell,\sigma) = \frac{1}{2}(p_\ell^2 + p_\sigma^2) + W(\ell,\sigma)\,. \qquad (4.6)$$

The two-dimensional space (ℓ,σ) may be viewed as a tensor product of two one-dimensional spaces $\ell \oplus \sigma$. The Hamiltonian and the density matrix in such a space are

represented by four-dimensional matrices. To use the standard methods for diagonalization and for propagation, we represent them as two-dimensional matrices using the following standard notation: the tensor product of a m by n matrix A with a m' by n' matrix B is an mm' by nn' matrix C with entries:

$$C_{(i-1)m'+k,(j-1)n'+l} = A_{i,j}B_{k,l}\,. \tag{4.7}$$

We denote the number of mesh points in ℓ direction as n_ℓ, in the σ direction as n_σ and the product space dimension as $n_{\ell\sigma}$. The resulting Hamiltonian matrix of dimension $n_{\ell\sigma} \times n_{\ell\sigma}$ is diagonalized, giving the eigenvalues E_n and the eigenfunctions ϕ_n, $n = 1, ..., n_{\ell\sigma}$. The resulting eigensystem is unique for each $\gamma_{\rm rel}$ and is calculated once. It is then used as a starting point for calculations at different temperatures.

Besides the diagonal matrix of $\boldsymbol{H}_s$, we need the matrices $\Sigma \equiv \langle\phi_{n'}|\boldsymbol{\sigma}|\phi_n\rangle$ and Σ^2 for calculation of the different commutators, cf. Eq.(3.2). Since the two-dimensional system vectors are stored and manipulated as a long one-dimensional vector, in practice $\boldsymbol{\sigma}$ is the column vector of length $n_{\ell\sigma}$ built out of n_ℓ column vectors $\sigma_1, ..., \sigma_{n_\sigma}$. The static shift χ vanishes in the symmetric system.

The number of energy states used in calculations depends on temperature and is much smaller than $n_{\ell\sigma}$. Actually, the convergence with respect to the number of energy levels used in calculations was checked and it was never necessary to use more that 30 levels for NM-QME and more that 100 for QME-CM. We estimate that our error bars are less than 10%.

V. RESULTS AND DISCUSSION

The derivation of the QME is based on perturbation theory and therefore is *a priori* limited to the weak damping regime. On the other hand, the fact that the treatment of the system is fully quantum allows for an exact zeroth order description in both the activated and the tunneling regime. To illustrate this we compare in Fig. 2 the temperature dependence of the logarithm of the quantum reaction rate constants for both our QME methods with the exact results of Topaler and Makri [4] and the centroid method of Shi and Geva [9]. For weak friction ($\gamma_{\rm rel} = 0.05$ and $\gamma_{\rm rel} = 0.1$), the agreement with the exact results is excellent for both NM-QME and QME-CM. For stronger friction, the NM-QME cannot reproduce the low-temperature behavior and the rates are strongly overestimated. However the QME-CM gives excellent agreement with the exact results over the entire temperature range, even for moderately strong friction ($\gamma_{rel} = 0.5$). Clearly, the collective mode representation has extended the applicability of the QME to significantly higher friction.

Comparing to centroid results of Shi and Geva, we note that although this version (marked as $k^{\varepsilon}_{\rm CiS}$ [9]) is a futher improvement of the centroid molecular dynamics method [8] and gives a good estimate of the high-friction rate constants at very low temperature, in the weak friction regime the rates are still underestimated.

Before we turn to comparison of the transmission coefficient as a function of friction, we make two remarks. First, we remind the reader that the transmission coefficient is a ratio of the quantum rate constant to the classical TST value $\kappa = k/k_{\rm TST}$. However, there is some ambiguity in what is meant by $k_{\rm TST}$ in the literature on quantum rate constants. Therefore, when comparing to the results of different methods one needs to pay attention to the definition of $k_{\rm TST}$ used, as it may slightly affect the resulting values of κ. As we plan to compare with the results of three calculations: Topaler and Makri [4], Liao and Pollak [10] and Shi and Geva [9], we review here the definition of $k_{\rm TST}$ used in each of these works.

The definition of $k_{\rm TST}$ is

$$k_{\rm TST} = \frac{1}{2\pi\hbar}\frac{k_B T}{Z}e^{-\beta E_b} \approx \frac{\omega_0}{2\pi}e^{-\beta E_b}.$$

Note that the last equality is approximate, as the ratio on the LHS in general has a small temperature dependence while the ratio on the RHS does not. The exact for $k_{\rm TST}$ (the LHS) was used in [4] while the approximate form (the RHS) was used by [10] and by us, below, for both NM-QME and QME-CM.

The definition of $k_{\rm TST}$ in [9], Eq.(24), is different:

$$k^{\rm TST}_{\rm cl} = \frac{1}{m}\frac{\langle\delta(s)ph(s)\rangle}{\langle 1 - h(s)\rangle},$$

where s is the reaction coordinate, p is the momentum, $h(s)$ is the Heaviside function and the averaging is over the classical many-body Boltzmann distribution.

The second comment is related to the spectral density used in the calculations. The exact results of Topaler and Makri [4] are obtained with the Ohmic spectral density with exponential cut-off (3.9). We used this spectral density in our NM-QME calculations. However, as was already mentioned in Sect III B, we could not use it for the QME-CM method as it does not allow analytic inversion of the Laplace transform of the new bath friction kernel. Instead, we used the Drude spectral density (3.10), which has a longer high-frequency tail. It is not clear *a priori* that the resulting rates will be the same, although the difference is not expected to be large. In the temperature dependence of the rates (Fig.2) the logarithmic scale emphasizes the orders of magnitude, not the specific numbers. It is not so for the transmission coefficient, which is a much more sensitive measure. In Fig.3 we compare the transmission coefficients calculated using the two different spectral densities. These calculations were done with the NM-QME method, since it is compatible with any form of the spectral density. ¿From Fig. 3 it is evident that at high temperatures (T=300K) the difference amounts to a downward shift by about 0.05 in the whole range of frictions we used. At lower temperatures, the difference has a more complicated behavior: basically the Drude spectral density gives a larger κ

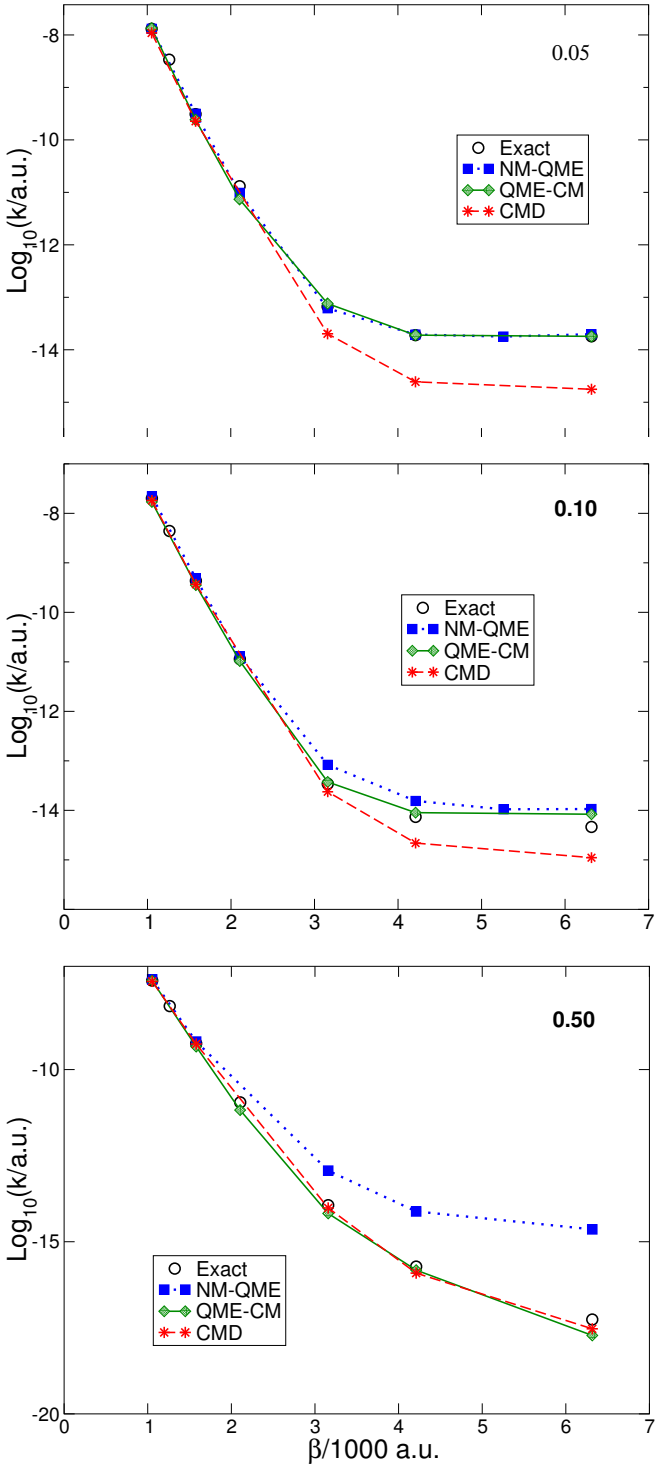

FIG. 2: The temperature dependence of the reaction rates for three frictions: Upper panel: $\gamma_{\rm rel} = 0.05$; Middle panel: $\gamma_{\rm rel} = 0.1$; Lower panel: $\gamma_{\rm rel} = 0.5$. The circles stand for exact results [4], the dashed line with stars denote centroid results, marked as $k^c_{\rm CIS}$ in [9], dotted line with squares - NM-QME results and solid line with shaded diamonds denote QME-CM

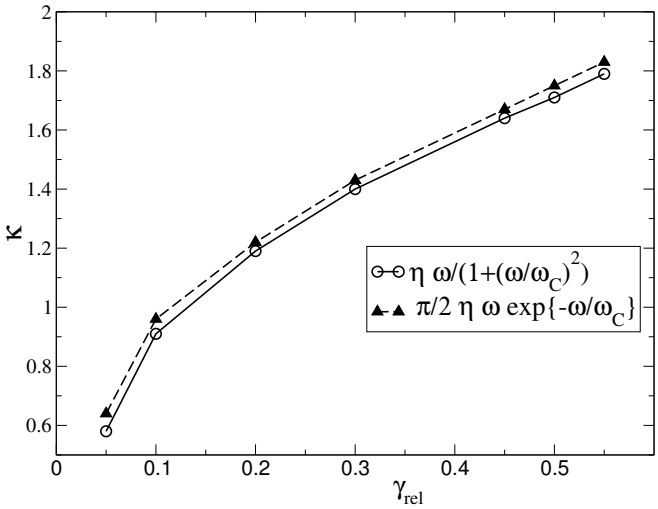

FIG. 3: The quantum transmission coefficient as a function of dimensionless friction at T=300K for NM-QME for two spectral densities: Drude (solid line with circles) and Ohmic with exponential cut-off (dashed line with triangles).

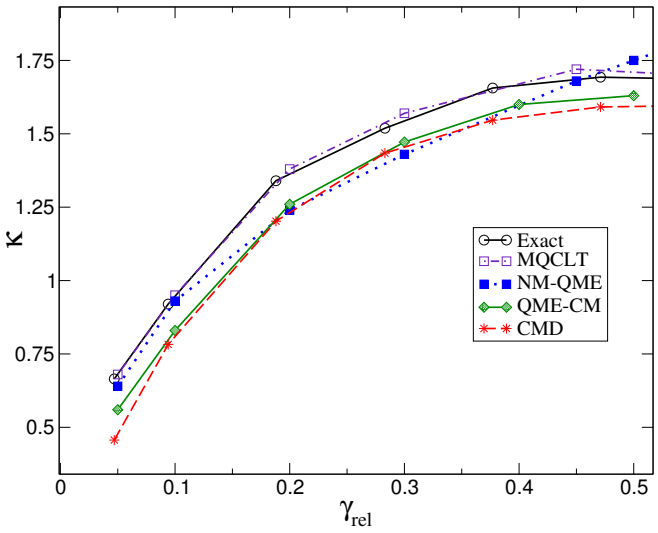

FIG. 4: The quantum transmission coefficient as a function of dimensionless friction at T=300K. The results are shown for exact [4], centroid $k^c_{\rm CIS}$ [9], MQCLT [10], NM-QME and QME-CM, as denoted in the legend.

than the Ohmic spectral density for weak friction and a smaller κ for strong friction. The value of the difference is however of the same order of magnitude as for high temperature. We will bear this in mind when analyzing κ as a function of friction.

In Fig.4, the weak friction part of the $\gamma_{\rm rel}$-dependence of the transmission coefficient is shown for T=300K. The MQCLT results demonstrate an excellent agreement with the exact results in this region. For weak friction ($\gamma_{\rm rel} \leq 0.1$) NM-QME shows very good accuracy too. However, for stronger friction, the results are less accurate and it fails to reproduce the turnover correctly. The

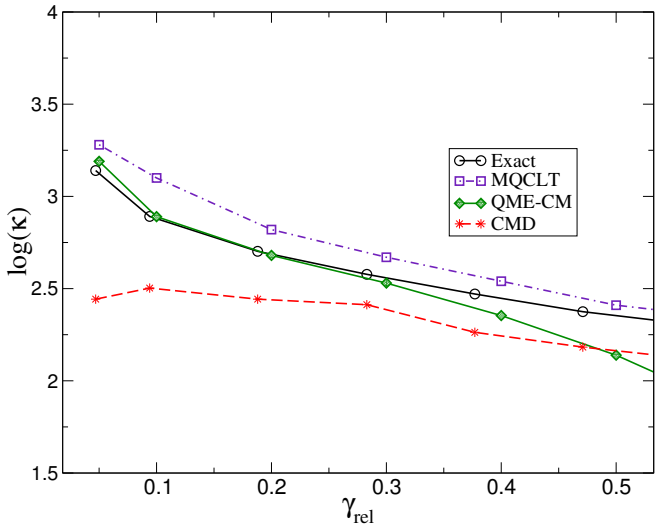

FIG. 5: The logarithm of the quantum transmission coefficient as a function of dimensionless friction at T=100K. The results are shown for exact [4], centroid $k^c_{\rm CIS}$ [9], MQCLT [10] and QME-CM, as denoted in the legend.

correct behavior is recovered in QME-CM. The transmission coefficient is slightly lower than the exact results, but recall that this is expected since we used the Drude spectral density which gives lower values of κ at this temperature. We therefore consider the agreement between the exact and QME-CM results to be quite satisfactory. The centroid results are also slightly lower that the exact ones, but the turnover is correctly reproduced.

For lower temperature (T=100K; Fig. 5) the turnover was shifted to vanishingly small $\gamma_{\rm rel}$. The MCQLT and centroid results frame the exact results from above and from below. As we already mentioned, NM-QME strongly overestimates the rates at low temperatures, so we do not show it in this figure. However, for QME-CM the agreement is again remarkable. Althought we consider the closeness of the points to the exact ones for $0.1 \leq \gamma_{\rm rel} \leq 0.3$ as accidential, the general behavior is fully reproduced. Recalling that at this temperatures the Drude spectral density pushes rates up for weak friction and down for stronger friction, we have an excelent agreement, demonstrating that the tunneling effects are fully accounted for in this method.

For even stronger friction $\gamma_{\rm rel} \geq 0.5$ the rates are underestimated and futher work is needed to extend the range of applicability of the method to stronger friction.

VI. CONCLUSIONS

In conclusion, we have calculated quantum reaction rates using the non-Markovian QME and its collective mode formulation. In the very weak fricton limit both methods give excellent agreement with the exact results in the whole temperature range. The QME-CM version extends the range of applicability of the method to moderate friction $\gamma_{\rm rel} \leq 0.5$ and correctly reproduces the friction dependence at both high and low temperatures.

Acknowledgments

We are grateful to Eli Pollak for fruitful discussions.

[1] P.G. Wolynes, Phys. Rev. Lett., **47**, 68 (1981)
[2] R.F. Grote and J.T. Hynes, J. Chem. Phys., **73**, 2715(1980)
[3] I. Rips and E. Pollak, Phys. Rev. A, **41**, 5366 (1990).
[4] M. Topaler and N. Makri, J. Chem. Phys. **101**, 7500 (1994).
[5] R.P. Feynman and F.L. Vernon Jr., Ann. Phys. **24**, 118 (1963).
[6] U. Weiss, *Quantum dissipative systems* (World Scietific, London, 1993) .
[7] N. Makri, J. Phys. Chem A, **102**, 4414 (1999)
[8] E.Geva, Q. Shi and G. Voth, ,J. Chem. Phys. **115** 9209 (2001)
[9] Q. Shi, E. Geva, J. Chem. Phys., **116**,3223(2002)
[10] J-L Liao and E. Pollak, J. Chem. Phys. **116**, 2718 (2002).
[11] Ch. Meier and D. Tannor, J. Chem. Phys. **111**, 3365 (1999).
[12] E. Hershkovitz and E. Pollak, J. Chem. Phys. **106**, 7678 (1997).
[13] F. Haake, Springer Tracts Mod. Phys., **66**, 98 (1973).
[14] E.Pollak, J. Chem. Phys. **85**,865 (1986).
[15] A.M. Levine, M. Shapiro and E. Pollak,J. Chem. Phys. **88**,1959 (1988).
[16] E. Pollak, in *Dynamics of Molecules and Chemical reaction*, edited by J. Zhang and R.W. Wyatt (Dekker, New York, 1996), pp 617-669
[17] P. Hänggi, P. Talkner and M. Berkovec, Reviews in Modern Physics, **62**, 251 (1990)
[18] W.T. Pollard, A.K. Felts and R.A. Friesner, Advances in Chemical Physics, volume XCIII (1996). Edited by I. Progogine and A. Rice.
[19] T.Yamamoto and W. Miller, JCP, **118** ,2135 (2003)
[20] D. T. Colbert and W.H. Miller, J. Chem. Phys., **96** ,1982 (1992)